

---

# MULTISCALE DYNAMICAL INDICES REVEAL SCALE-DEPENDENT ATMOSPHERIC DYNAMICS

---

## Chenyu Dong

College of Design and Engineering  
National University of Singapore  
chenyu.dong@u.nus.edu

## Gabriele Messori

Department of Earth Sciences,  
Uppsala University, Sweden  
Swedish Centre for Impacts of Climate Extremes (climes),  
Uppsala University, Sweden  
Department of Meteorology and Bolin Centre for Climate Research  
Stockholm University, Sweden  
gabriele.messori@geo.uu.se

## Davide Faranda

LSCE, Université Paris-Saclay, France  
London Mathematical Laboratory, UK  
IPSL, École Normale Supérieure, France  
davide.faranda@lsce.ipsl.fr

## Adriano Gualandi

Department of Earth Sciences  
University of Cambridge  
Istituto Nazionale di Geofisica e Vulcanologia, Italy  
ag2347@cam.ac.uk

## Valerio Lucarini

School of Computing and Mathematical Sciences  
University of Leicester, UK  
v.lucarini@leicester.ac.uk

## Gianmarco Mengaldo\*

College of Design and Engineering  
National University of Singapore  
mpegim@nus.edu.sg

## ABSTRACT

Geophysical systems are inherently complex and span multiple spatial and temporal scales, making their dynamics challenging to understand and predict. This challenge is especially pronounced for extreme events, which are primarily governed by their instantaneous properties rather than their average characteristics. Advances in dynamical systems theory, including the development of local dynamical indices such as local dimension and inverse persistence, have provided powerful tools for studying these short-lasting phenomena. However, existing applications of such indices often rely on predefined fixed spatial domains and scales, with limited discussion on the influence of spatial scales on the results. In this work, we present a novel spatially multiscale methodology that applies a sliding window method to compute dynamical indices, enabling the exploration of scale-dependent properties. Applying this framework to high-impact European summertime heatwaves, we reconcile previously different perspectives, thereby underscoring the importance of spatial scales in such analyses. Furthermore, we emphasize that our novel methodology has broad applicability to other atmospheric phenomena, as well as to other geophysical and spatio-temporal systems.

**Keywords** Dynamical Indices · Multiscale · Atmospheric Dynamics · Heatwaves

# 1 Introduction

Since the seminal contributions by Lorenz [1, 2], it is well-known that as a result of the chaotic and multiscale nature of the atmospheric flow, the atmosphere has a limited horizon of predictability. It is also well-known that such predictability is very strongly-state dependent: certain configurations of the atmospheric flow are associated with higher instability than others, so that, at practical level, the skill of weather forecast often results to be more limited [3, 4]. Lyapunov exponents (LEs) provide a powerful framework for studying the overall stability properties of a complex system and of how well we can predict its evolution on average [5]. In addition, The celebrated Kaplan-Yorke formula allows one to link the spectrum of LEs of a dynamical system to a notion of dimension of its attractor [6, 7]. Yet, again, such a notion lacks information on the local properties of the attractor. To address the local properties of the attractor, the finite-time versions of LEs - FTLEs - were introduced [8]. These convey a measure of the local (in the phase space) stability properties of the system. Indeed, in the case of the atmosphere, the local variations in the instability of the flow can be quantified by looking at the fluctuations of the individual finite-time Lyapunov exponents and at the geometry of the tangent space [9, 10, 11]. However, approaches based on LEs, including FTLEs, are more suitable for problems where an equation-based model (or its approximation) is explicitly known.

Recent advances in dynamical systems theory have provided a mathematically rigorous, and purely data-driven framework (without the need to know the underlying equation-based model of the system) for analyzing local, instantaneous, state-dependent dynamical properties of complex systems. The data-driven framework is achieved by looking at the statistics of close recurrences of the orbit with respect to a reference state of interest [12, 13]. This has led to an data-efficient way to estimate the local dimension  $d$ , which, roughly speaking, provides local geometric information about the system's complexity by quantifying the number of active degrees of freedom deducible from the observations. Additionally, the analysis of recurrences has led to introducing a second index: the inverse of the persistence time ( $\theta$ ), which estimates the reciprocal of the local persistence time near the reference state.

Given their local nature in the phase space, they are particularly well-suited for studying transient behaviors, such as extreme events in geophysical systems. Indeed, these two indices have been applied to several geophysical problems, providing insightful analysis for temperature extremes and their atmospheric drivers [14, 15, 16], the life cycles and transitions of weather regimes [17, 18, 19], ocean variability [20] and earthquake dynamics [21].

The works just mentioned address the different phenomena they target looking at the system's dynamical behavior on a single and fixed spatial domain that is of interest to the specific study. This implies that the indices adopted for each study only 'see' one single and fixed spatial scale, approach that does not fully capture the possibly multiscale nature of several of these and other real-world dynamics. Indeed, many geophysical and other spatio-temporal systems exhibit dynamics that span a wide range of scales, both spatially and temporally; choosing a fixed region (i.e., spatial domain) might not fully account for these multiscale physical processes. In addition, pre-selecting a fixed spatial domain requires prior knowledge of the studied system and its dynamics, and may fail to account for dynamical processes originating in regions afar from the fixed domain selected (e.g., teleconnections in the context of atmospheric dynamics).

In fact, the limitations of the fixed-domain approach just outlined were also noticed by [22] in the study of tropical cyclones, where a Lagrangian perspective was proposed to better capture their dynamics. To address similar challenges, empirical mode decomposition (EMD) was recently applied to decompose a given system into components at different temporal scales, prior to calculating the local indices  $d$  and  $\theta$  [23, 24]. This approach reveals both the systems' scale-dependent dynamical characteristics and the interactions between different scales [23]. However, the application of EMD to systems with multiple spatio-temporal scales remains challenging, especially if the systems are high-dimensional. At the same time, another study on the dynamics of slow earthquakes divided the spatio-temporal system into multiple subsections based on predefined physical quantities, with the dynamical properties of each subsection characterized individually [25]. Despite various efforts in the existing literature to account for the multiscale nature of real-world systems, these methods are often tailored to specific systems, thereby calling for a more systematic approach.

In this work, we seek to overcome the above-mentioned limitations by developing a spatial multiscale approach that is able to uncover dynamical properties at different spatial scales. The new approach is tailored to complex spatio-temporal systems, and based on the framework of local dynamical indices  $d$  and  $\theta$  [12, 13]. We show that our approach is able to provide new dynamical insights for practical real-world complex problems. To this end, we apply our approach to European summertime heatwaves, that are high-impact events that have been extensively studied in the literature, thus providing an ideal testbed for our approach [26, 27, 28, 15, 29, 30]. In particular, we show how two diverging views can be reconciled using our approach.



## 2 A new approach to reveal scale-dependent dynamics

Grounded at the intersection of dynamical systems theory and extreme value theory, the two instantaneous dynamical indices which we adopt here were developed by [12] and [13] to characterize local dynamical properties of complex systems. Within this framework, for each given state of interest  $\zeta$ , two indices—termed local dimension ( $d$ ) and inverse persistence ( $\theta$ ), can be computed based on the recurrences of  $\zeta$  (i.e., when the system visits states neighboring  $\zeta$  in the phase space). The local dimension  $d$  can be considered a proxy for the number of active degrees of freedom of the system locally around  $\zeta$ . It therefore reflects the complexity of the dynamics near the state  $\zeta$ ; if a system has more active degrees of freedom, its complexity is greater. The inverse persistence ( $\theta$ ) is derived from the extremal index, which is defined in extreme value theory to measure the clustering of extremes. For a given state  $\zeta$ ,  $\theta$  can be interpreted as a measure of the inverse of the system’s persistence time near that state and is defined between 0 and 1. A high value of  $\theta$  indicates that the system will quickly leave the neighborhood of  $\zeta$ , while a value of  $\theta$  close to 0 suggests that the system will persist in states resembling  $\zeta$ . Both  $d$  and  $\theta$  can be related to the intrinsic predictability of the system at a specific time [31]. States with high local dimension ( $d$ ) and high inverse persistence ( $\theta$ ) are usually considered less predictable due to their complex and fast dynamics. This has been partly confirmed by [32] for both idealized and real-world datasets through a new instantaneous index that directly measures predictability within the same theoretical framework. In atmospheric applications, these dynamical indices can be computed for each instantaneous state of the atmosphere, as represented by one or more variables (e.g., a given sea-level pressure map over a given geographical domain). A more detailed description of these indices can be found in the SI Section 1, with the full mathematical derivation provided in [33]. However, it is important to acknowledge that the computation of these dynamical indices relies on assumptions that are not fully respected by the data we use, such as stationarity and hyperbolicity. The effect of this is difficult to quantify, since the framework we adopt is problematic to falsify [34].

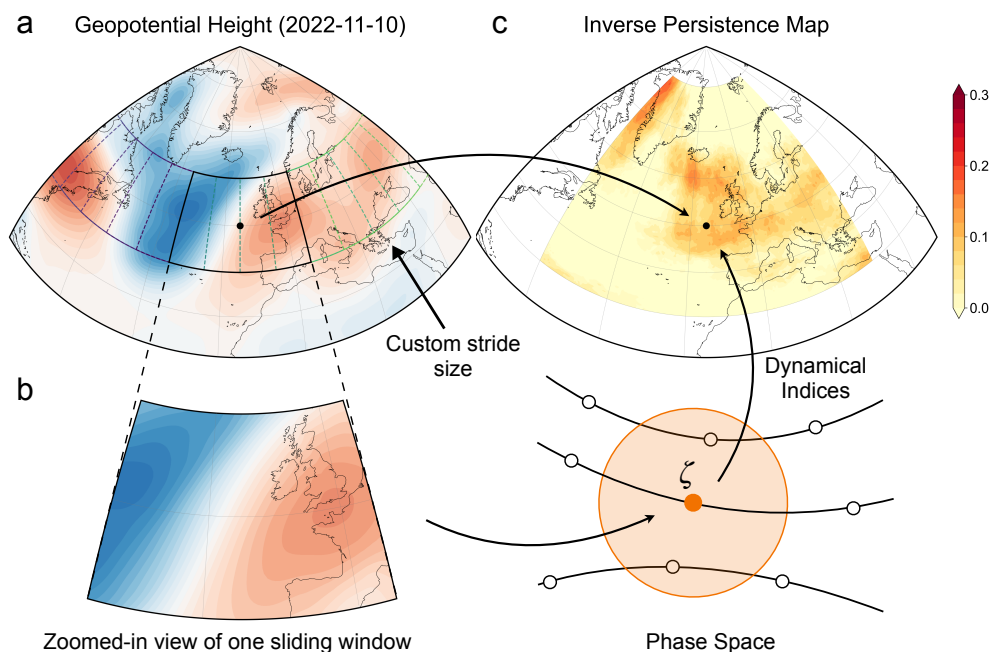


Figure 1: **Schematic illustration of the computational framework for scale-dependent dynamical indices.** (a) An example of the 500hPa geopotential height map from 2022/11/10, with bounding boxes showing sliding windows spaced at uniform stride size. (b) Zoomed-in view of a sliding window and its associated idealized schematic phase space illustration. The orange dot  $\zeta$  represents the state in the specific sliding window and the orange circle corresponds to neighborhood of  $\zeta$  in the phase space, which is used to define recurrences and compute dynamical indices (see Materials and Methods). (c) The map of inverse persistence  $\theta$ . The edges of the figure are left blank because the center of the sliding windows do not extend to those regions.

Here, we propose a novel spatially multiscale approach that computes dynamical indices using a moving window scheme, as depicted in Fig. 1. Unlike the traditional approach that considers the entire spatial domain (i.e., the entire geographical map in the case of weather applications, such as the one depicted in Fig. 1) as a state in the phase space, we treat each small map within the sliding window separately (Fig. 1a), and compute the associated dynamical indices

(Fig. 1b) for each small map. Therefore, instead of obtaining one numerical value for  $d$  and one for  $\theta$  for the whole map, we obtain numerical values for each sliding window map for both  $d$  and  $\theta$ . By assigning these values to the center of the sliding window map, and considering sliding windows covering the whole region of interest, we obtain spatial maps of the dynamical indices (Fig. 1c). This makes the dynamical indices not only ‘local’ in the phase space (i.e., instantaneous in time) but also spatially (i.e., geographically) ‘local’, features that can provide valuable insights. While we acknowledge that these subsystems are not strictly independent, we proceed with this division as these dynamical indices have proven effective for relatively localized systems [31].

In Fig. 1, we use a window size of  $40^\circ$  longitude by  $20^\circ$  latitude as an example, while emphasizing that the window size can be customized to capture dynamics at different scales of interest. Similarly, our use of the Euro-Atlantic region here is for illustration purposes only – our method can be extended to the entire globe, enabling the study of e.g., teleconnections in the context of weather and climate applications. It is worth noting that our framework shares structural and objective similarities with convolutional kernels from computer vision [35], which are also widely used in atmospheric dynamics studies [36, 37, 38]. Both approaches employ a sliding window technique to extract scale-dependent information from data, with one grounded in dynamical system theory and the other in machine learning.

### 3 A Real-World Case Study

#### 3.1 European Summertime Heatwaves

To show the advantages of the new approach, we focus on European summertime heatwaves. These complex phenomena can pose a substantial threat to society and ecosystems [39, 40], and it is critical to enhance our understanding of their dynamics for improving prediction capabilities and mitigating their impacts [41, 42]. European summer heatwaves are driven by different processes and show significant inter-regional differences [28]. In higher-latitude regions, European summer heatwaves are often associated with atmospheric blocking, which results in adiabatic warming from subsidence and clear-sky conditions [42, 43, 30]. At lower latitudes, European summer heatwaves are linked to persistent subtropical ridges, a configuration that weakens zonal flow and strengthens meridional flow, facilitating the southerly advection of hot air into southern Europe [44]. From a traditional meteorological dynamics perspective, both blocking and subtropical ridges are highly persistent atmospheric configurations [45]. However, recent studies based on dynamical systems theory have only found a weak to moderate connection between anomalously persistent circulation patterns in the mid-troposphere and summertime heatwaves, and few significant persistence anomalies of the surface circulation patterns [15]. Meanwhile, earlier studies based on dynamical indices [13, 46], along with other research [47, 48], have argued that blocking is a transient feature of the atmospheric system, characterized by high instability and low predictability. These conclusions differ markedly from the traditional meteorological perspective and call for a reconciliation of these divergent views. In section 4, we show how our new approach can address these divergent views and enrich our dynamical understanding of these phenomena.

#### 3.2 Data

In this study, we used state-of-the-art ERA5 reanalysis daily mean data from 1979 to 2022 [49]. The scale-dependent dynamical indices analysis is performed on both sea level pressure (SLP) and 500-hPa geopotential height (Z500), two variables extensively used to analyze circulation patterns associated with temperature extremes [15, 50, 51]. We have computed the dynamical indices for the entire Northern Hemisphere ( $180^\circ\text{W}$ - $180^\circ\text{E}$ ,  $0^\circ$  to  $90^\circ\text{N}$ ), with the data downsampled from the original resolution of  $0.25^\circ$  to  $0.5^\circ$  to reduce computational costs. The stride size for the sliding window is set to  $0.5^\circ$  in both the longitude and latitude directions. In the main text, we present results using a window size of  $40^\circ$  longitude by  $20^\circ$  latitude, while the results for a smaller window size ( $20^\circ$  longitude by  $10^\circ$  latitude) are provided in the Supplementary Information. Previous studies have shown that the dynamical systems metrics are dependent on the studied domain and also exhibit a strong seasonal cycle [13]. Recognizing this, we deseasonalize and standardize both dynamical indices before further interpreting the results. The seasonal cycle is calculated as the mean of a 31-day moving window centered on each calendar day, while standardization is performed on a grid-point-by-grid-point basis. For all mean values of standardized anomalies presented in this paper, we assess statistical significance using the 95% confidence interval generated by a bootstrap test with 1,000 resamples (with replacement). To control the multiple-testing issue in spatial maps, we apply the Benjamini-Hochberg procedure following [52].

We define regional summertime heatwaves over the British Isles, Scandinavia, central Europe (Germany), Iberia, and the central Mediterranean for extended summer season (JJAS), following the bounding boxes used in [28]. We then identify heatwave occurrences using the procedure outlined in [29], with the detailed steps provided in Supplementary Information.

## 4 Results

### 4.1 Scale-dependent circulation dynamics during heatwaves

In Fig. 2, we present the composite maps of the standardized anomalies of dynamical indices for the onset days of European summertime heatwaves (we will use heatwaves hereafter, for the sake of brevity, when referring to European summer heatwaves). We computed the dynamical indices using SLP (Fig. 2, rows 1 and 2) and Z500 (Fig. 2, rows 3 and 4) separately to show the distinct dynamical behavior of the surface-level and mid-level troposphere, following [15]. The composite maps of the standardized anomalies of the dynamical indices derived from the two observables reveal clear differences in both magnitude and spatial configuration, with the Z500-based indices generally showing stronger anomalies.

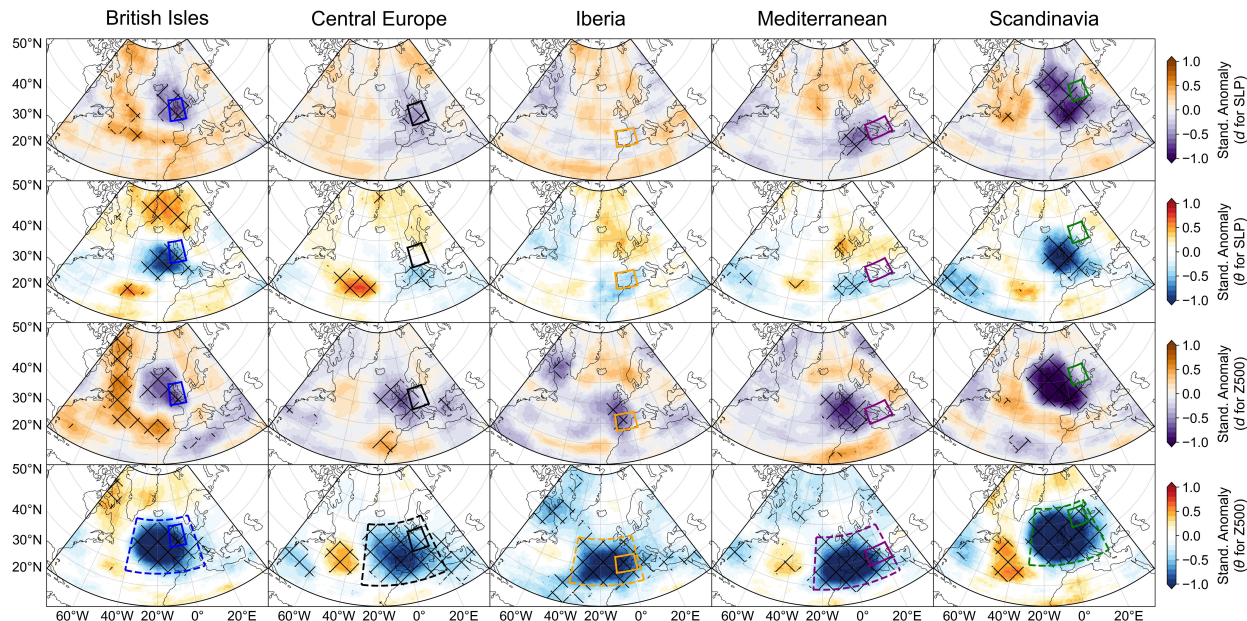


**Figure 2: Composite of standardized anomalies of dynamical indices for the onset days of European summertime heatwaves.** Composite of standardized anomalies for the local dimension  $d$  (rows 1 and 3) and the inverse persistence  $\theta$  (rows 2 and 4) that were computed using both SLP (rows 1 and 2) and Z500 (rows 3 and 4). Each column represents heatwaves over a specific region, with the affected area indicated by a colored solid bounding box. The dashed bounding boxes in the last row highlight regions utilized in the analysis presented in Fig. 4. The regions studied are as follows: British Isles (blue; solid box:  $49^{\circ}\text{N}$ – $59^{\circ}\text{N}$ ,  $10^{\circ}\text{W}$ – $2^{\circ}\text{E}$ ; dashed box:  $36^{\circ}\text{N}$ – $62^{\circ}\text{N}$ ,  $40^{\circ}\text{W}$ – $10^{\circ}\text{E}$ ), Central Europe (black; solid box:  $45^{\circ}\text{N}$ – $55^{\circ}\text{N}$ ,  $4^{\circ}\text{E}$ – $16^{\circ}\text{E}$ ; dashed box:  $30^{\circ}\text{N}$ – $60^{\circ}\text{N}$ ,  $30^{\circ}\text{W}$ – $20^{\circ}\text{E}$ ), Iberian Peninsula (orange; solid box:  $36^{\circ}\text{N}$ – $44^{\circ}\text{N}$ ,  $10^{\circ}\text{W}$ – $3^{\circ}\text{E}$ ; dashed box:  $30^{\circ}\text{N}$ – $53^{\circ}\text{N}$ ,  $38^{\circ}\text{W}$ – $5^{\circ}\text{E}$ ), Mediterranean (purple; solid box:  $36^{\circ}\text{N}$ – $44^{\circ}\text{N}$ ,  $10^{\circ}\text{E}$ – $25^{\circ}\text{E}$ ; dashed box:  $28^{\circ}\text{N}$ – $54^{\circ}\text{N}$ ,  $25^{\circ}\text{W}$ – $25^{\circ}\text{E}$ ), and Scandinavia (green; solid box:  $57^{\circ}\text{N}$ – $65^{\circ}\text{N}$ ,  $25^{\circ}\text{E}$ – $20^{\circ}\text{E}$ ; dashed box:  $40^{\circ}\text{N}$ – $67^{\circ}\text{N}$ ,  $30^{\circ}\text{W}$ – $24^{\circ}\text{E}$ ). Cross-hatching indicate statistical significance.

In the mid-level troposphere, significant negative  $\theta$  anomalies (Fig. 2, row 4) are observed for Z500 slightly west of the target regions. This suggests that during the onset days of heatwaves, the upstream atmospheric configuration of the affected regions is unusually persistent, but other regions in the Euro-Atlantic sector do not have increased persistence. Indeed, less persistent atmospheric configurations with relatively smaller spatial extent can be found over the Atlantic Ocean for all studied regions (except Iberia). We note that the results presented in Fig. 2 are robust with respect to the sliding window size, as similar spatial anomaly patterns are observed when a smaller sliding window is applied (see SI Fig. S1).

In addition, the local dimension ( $d$ ) of Z500 (Fig. 1, row 3) shows some negative anomalies that are co-located with, but weaker than, the negative anomalies of inverse persistence ( $\theta$ ). Other regions display relatively weak or near-zero anomalies, except for British Isles heatwaves, that exhibit a strong positive anomaly over the Atlantic. Such results suggest that Z500 patterns display reduced dynamical complexity during heatwave onset days near the affected regions. The results for  $\theta$  and  $d$  on Z500 together support the view that European summertime heatwaves are accompanied by persistent and low-dimensional atmospheric configurations in the mid-troposphere from a dynamical systems perspective.

At the surface level, we note that the standardized anomalies are less pronounced, yet still reveal some coherent patterns (Fig. 2). For heatwaves occurring outside Iberia, we observe significant negative anomalies in both local dimension ( $d$ ) and inverse persistence ( $\theta$ ) near the affected regions, similar to those in the mid-level atmosphere, although much weaker. In Iberia, no such significant anomalies are observed for  $\theta$  over the entire domain. It is particularly noteworthy to observe distinct dynamical properties at the surface and mid-level troposphere, as also noted by [15], especially since these differences are not evident in the composite anomaly maps of the raw variables (see SI Fig. S2). This is also consistent with meteorological perspectives, as heat lows can develop during heatwaves [53], exhibiting dynamics that differ significantly from the mid-tropospheric flow. At the same time, previous studies have shown that blocking events, which are frequently associated with heatwaves, are primarily reflected at the mid- or upper-level flows [54, 55].

Considering the importance of blocking and the non-systematic link between heatwaves and blocking, we further extend our analysis to blocking events to enhance the completeness of this study, particularly given previously noted contrasting perspectives on their dynamical properties. From a meteorological perspective, blocking events are persistent atmospheric configurations by definition [43, 54, 55]. However, recent studies grounded in dynamical systems theory propose a differing view, suggesting that blocking regimes are not inherently persistent atmospheric configurations [13, 17]. In order to reconcile differing these views, we apply a blocking detection algorithm to examine the dynamical properties of blocking following [56], with detailed steps provided in SI Text S3. We find that, regardless of their location, blocking events are associated with geographically localized more persistent (low  $\theta$ ) and less complex (low  $d$ ) mid-level tropospheric flows – see SI Fig. S5, where the second and third rows represent the anomalies of  $d$  and  $\theta$  for the blocking events identified by the blocking algorithm adopted. Yet, regions surrounding the blocking center are less persistent (high  $\theta$ ) and more complex (high  $d$ ), and may be less predictable as also shown in operational forecasts [55], and in agreement with the theoretical arguments set in [47]. This further analysis on blocking, bridges the two seemingly different views that were present in the literature, thereby showing how the new approach can capture relevant informative features of atmospheric dynamics.

A further fascinating aspect emerges when looking at the temporal coherence of the anomaly fields of the dynamical indicators (as well as the meteorological fields themselves) as we approach the onset of the heatwaves and as we observe its decay, see Figs. S3-S5 in the SI. In [57, 58] it was argued, on the basis of large deviation theory, that persistent extreme events like heatwaves and cold spells are characterized by dynamical typicality. This means that the occurrence of the extreme event or interest - e.g. heatwave in the British isles - requires a very special large-scale configuration of the atmospheric fields, which to a very good degree of approximation repeats itself, thus defining a class of analogues, for different individual occurrences of the event. In other terms, Such a configuration is atypical with respect to the overall statistics of the fields, but becomes typical when we focus on the days associated with the heatwave of interest. Additionally, it was argued that special large-scale structures coherently evolve in the period leading to the onset of the extreme event. A separate confirmation of this idea was given on the 2021 Pacific Northwest heatwave by [59]. Indeed, we find that in the days preceding the onset of the heatwaves the composite fields have a rather high degree of coherence, providing good evidence for the existence of a *highway* in phase space (technically associated with an instantonic trajectory) leading to the events; see discussion in [60] and first original contribution is this direction in [61]. Note that such coherence is largely lost after the decay of the heatwaves, because the lysis process, as opposed to the onset, does not follow a preferential path.

## 4.2 A richer dynamical view

To further complement our analysis with the new framework, we conducted a comparative study following the previous single-domain approach – treating the entire Euro-Atlantic domain as a single dynamical system. Fig. 3 presents box plots of standardized anomalies of dynamical indices for the entire Euro-Atlantic domain during the onset days of summertime heatwaves, with each subplot corresponding to a specific column (i.e., affected region considered) in Fig. 2. Unlike our new approach in Fig. 2, that shows significant anomalies for both  $d$  and  $\theta$  in all regions considered, the single-domain approach shows that significant results are achieved in only three cases (out of twenty). This suggests that atmospheric patterns associated with heatwaves exhibit a range of different dynamical properties, that are difficult to capture via the single-domain approach. Specifically, using the single-domain method, at the mid-level, both the British Isles and Central Europe exhibit near-zero standardized anomalies, whereas the other three regions display negative anomalies for both indices. However, only the inverse persistence ( $\theta$ ) for the Iberian Peninsula and the Mediterranean is statistically significant. At the surface level, no significant results are observed, except for the SLP-based inverse persistence ( $\theta$ ), which shows positive standardized anomaly over the British Isles.

These results are consistent with [15], showing that summertime heatwaves in Europe are not systematically linked with more persistent large-scale circulation patterns. We do not consider this to be in conflict with the findings from our new approach (Fig. 2); rather, it underscores the importance of incorporating different spatial scales in the analysis. Our new approach can pinpoint the regions that exhibit the most dynamical relevance of the studied phenomena, a result that

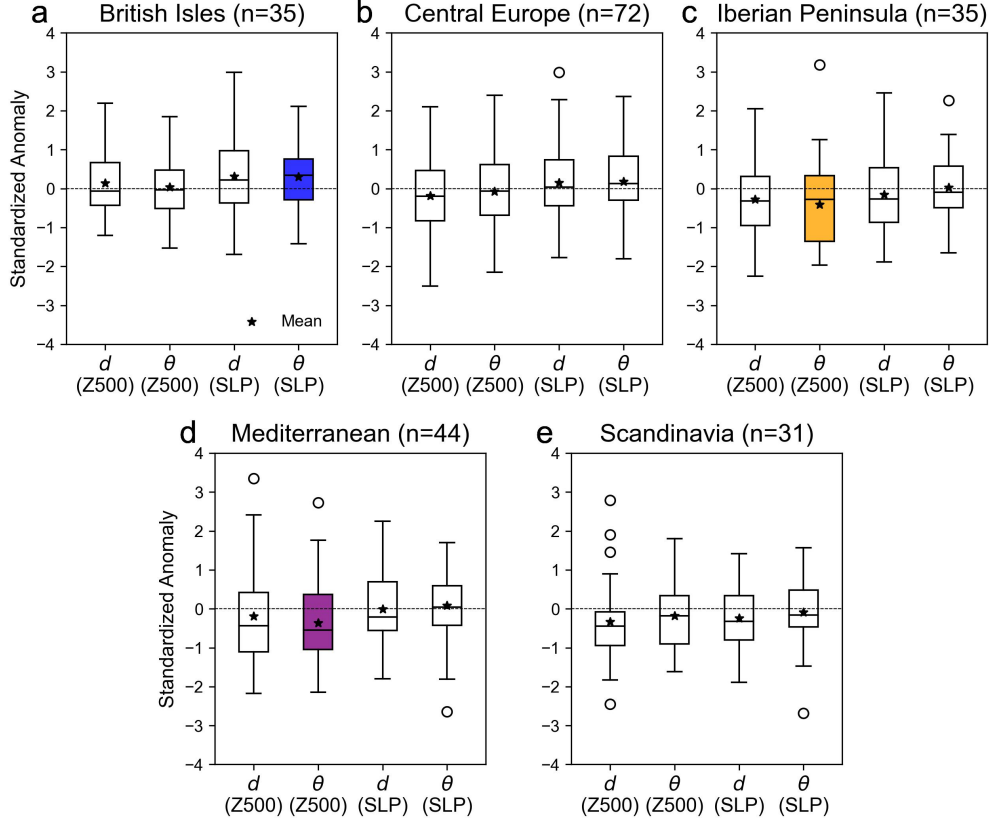


Figure 3: **Box plots of standardized anomalies of dynamical indices for the Euro-Atlantic sector using the single-domain approach.** The dynamical indices are computed within the large-scale bounding box ( $20^{\circ}\text{N}$ – $80^{\circ}\text{N}$ ,  $80^{\circ}\text{W}$ – $40^{\circ}\text{E}$ ), followed by standardization steps as described above. Each subplot shows the results for one studied region, with statistically significant results highlighted in the color representing that region, as in Fig. 1. The ends of the boxes indicate the 25th and 75th percentiles, while the whiskers extend to 1.5 times the interquartile range beyond the box.

was not possible to achieve with the pre-selected fixed-domain approach. Indeed, based on the results shown in Fig. 2, we can identify bounding boxes where the mid-level atmosphere demonstrates significantly higher persistence (dashed bounding boxes in row 4, Fig. 2). Different bounding boxes are used for heatwaves in different affected regions, as expected due to the assumption that events in different regions may have diverse atmospheric drivers. We compute the dynamical indices of atmospheric circulation patterns within each bounding box, and plot the standardized anomalies as box plots for the heatwave onset days in the corresponding regions (see Fig. 4). Consistent with expectations, more statistically significant results are observed when smaller bounding boxes are used. In particular, significantly more persistent characteristics are displayed at the mid-level troposphere during the onset days of heatwaves for all regions. Similarly, negative anomalies in local dimension ( $d$ ) are observed across all regions, although they are statistically significant only in the Mediterranean and Scandinavia. At the surface level, only the local dimension ( $d$ ) in Scandinavia exhibits a significant negative anomaly, while the others are not significant.

## 5 Discussions and conclusions

By collectively examining the results discussed above, we can recognize the importance of spatial scales in studies based on dynamical indices. Although European heatwaves are not systematically linked with large-scale persistent atmospheric circulation patterns, they are accompanied by significant localized dynamical characteristics, as revealed by the new methodology introduced in this study. Furthermore, we demonstrate that the guidance provided by this method can be combined with the fixed-domain approach to select bounding boxes better suited to the studied phenomena.

Dynamical systems theory has been extensively applied to diverse complex physical systems across various spatial scales [33, and references therein]. However, when addressing spatio-temporal systems, past studies have computed the



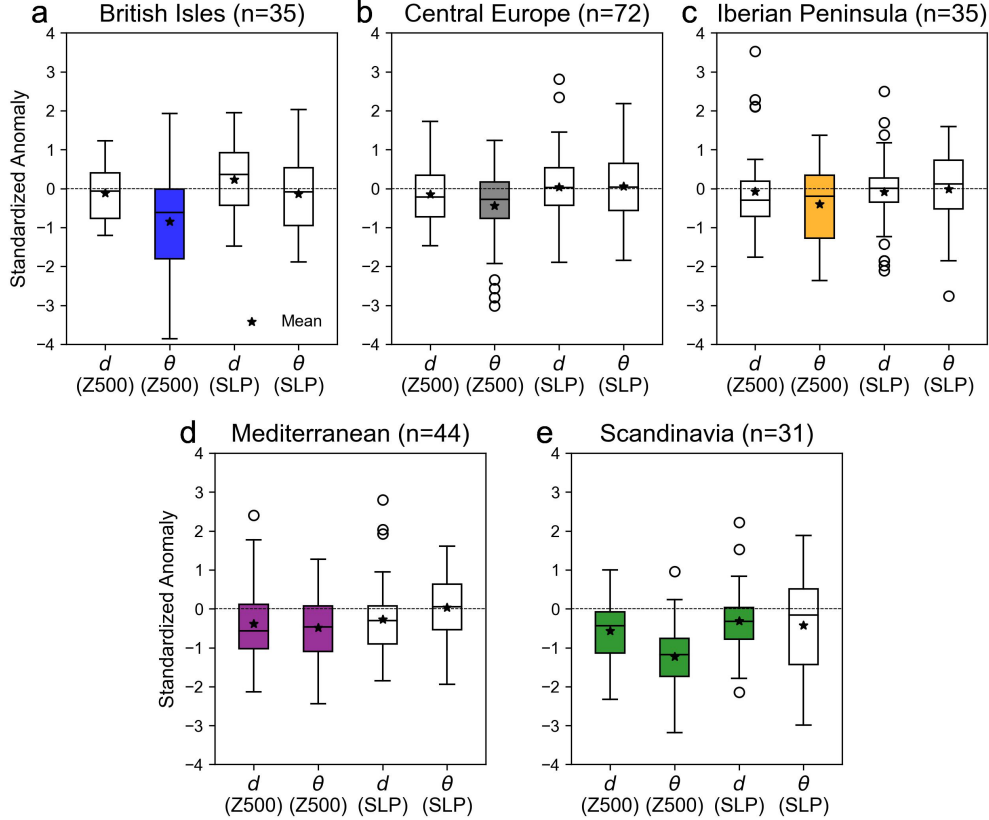


Figure 4: **Box plots of standardized anomalies of dynamical indices for the dashed bounding boxes shown in Fig. 2 using the single-domain approach.** The dynamical indices are computed within the the dashed bounding boxes shown in the row 4 of Fig. 2, followed by standardization steps as described above. Each subplot shows the results for one studied region, with statistically significant results highlighted in the color representing that region, as in Fig. 1. The ends of the boxes indicate the 25th and 75th percentiles, while the whiskers extend to 1.5 times the interquartile range beyond the box.

metrics on a predefined bounding box based on prior expert knowledge. While sensitivity analyses on the boundaries of such bounding boxes are often discussed, the influence of the bounding box’s size – namely, the considered spatial scale – is rarely examined. To address these constraints, we propose a novel framework for applying dynamical indices to spatio-temporal complex systems, inspired by the concept of convolutional neural networks that leverage localized filters to extract spatially and temporally relevant features. By employing a sliding bounding box with a customizable size, we extract the system’s dynamical properties that are ‘local’ in both time (i.e., instantaneous) and space (i.e., spatially specific) at the spatial scale of interest. Compared to the previous approach with only two indices as outputs, this method generates spatio-temporal maps that allow for a more detailed analysis, providing richer insights into the dynamical features of certain phenomena of interest.

In this work, we applied this new framework to high-impact European summertime heatwaves to demonstrate its effectiveness. Our results offer an explanation that reconciles the previously noted discrepancy in the persistence of heatwaves-associated circulation patterns between the meteorological view and the dynamical systems theory perspective [15]. In fact, the conclusions drawn from both perspectives are valid within their respective contexts, where the glue between the two is provided by the varying dynamical characteristics of heatwaves across different spatial scales. Although heatwaves are not systematically linked to large-scale circulation patterns with distinct dynamical properties, they often display significant persistence and low-dimensional signatures in the regions upstream of the affected areas. Additionally, looking at the temporal evolution of the anomaly fields of the dynamical indicators and of the meteorological fields themselves we find further confirmation of the validity of the notion of dynamical typicality of persistent extreme events discussed in [57, 58].

More broadly, we extended our analysis to summertime blocking events that frequently cause heatwaves in Europe, a phenomenon considered highly persistent by definition but, according to some recent studies employing various methodologies – including dynamical systems theory [13, 46], mathematical models [47], and ensemble forecasts [62] – is regarded as a relatively unpredictable configuration. Similar to the findings for heatwaves, we observed that blocking centers exhibit significantly greater persistence and predictability, while being accompanied by configurations with contrasting dynamical properties in other regions within the Euro-Atlantic sector. This indicates that the dynamical properties of blocking are closely tied to spatial scales, and analyses at different spatial scales have resulted in divergent conclusions in previous studies [45, 13]. Thus, we believe that our approach bridges the perspective of dynamical systems theory and more conventional meteorological views, providing an explanation for the divergent result present in the literature.

As a novel framework, we anticipate its broad application in future research rooted in dynamical systems theory, as it is general in nature and can be applied to any region or variable in atmospheric dynamics, as well as other geophysical systems (e.g., slow earthquakes [25]). For instance, it could be utilized to study energy cascades [63] in turbulent flow to better understand the transfer of energy across different scales. In atmospheric science, we believe it has the potential to open up research opportunities for a deeper understanding of teleconnection dynamics [64], as our analysis provides spatio-temporal dynamical information. At the same time, the temporal evolution of dynamical indices, which has been studied in the life cycles of weather regimes [18, 17] and extreme events [14], can be further complemented by our framework to provide additional insights. Moreover, it could potentially be used to identify distant dynamical precursors of the studied phenomena – another aspect that cannot be achieved using the fixed-domain approach. This holds great significance for advancing our understanding of their onset mechanisms and potentially enhancing predictive modeling.

## Acknowledgments

G.M. acknowledges support from MOE Tier 2 grant no 22-5191-A0001-0, titled: ‘Prediction-to-Mitigation with Digital Twins of the Earth’s Weather’. V.L. acknowledges the support provided by the Horizon Europe Project ClimTIP (Grant No. 100018693) and by the EPSRC project LINK (Grant No. EP/Y026675/1).

## References

- [1] E. N. Lorenz. The predictability of a flow which possesses many scales of motion. *Tellus*, 21:289–307, 1969a.
- [2] E. N. Lorenz. Three approaches to atmospheric predictability. *Bull. Am. Meteorol. Soc.*, 50:345–349, 1969b.
- [3] T N Palmer. Predicting uncertainty in forecasts of weather and climate. *Reports on Progress in Physics*, 63(2):71–116, jan 2000.
- [4] Julia Slingo and Tim Palmer. Uncertainty in weather and climate prediction. *Philosophical Transactions of the Royal Society A: Mathematical, Physical and Engineering Sciences*, 369(1956):4751–4767, 2011.
- [5] Arkady Pikovsky and Antonio Politi. *Lyapunov exponents: a tool to explore complex dynamics*. Cambridge University Press, 2016.
- [6] James L. Kaplan and James a. Yorke. Preturbulence: A regime observed in a fluid flow model of Lorenz. *Communications in Mathematical Physics*, 67(2):93–108, 1979.
- [7] Jean-Pierre Eckmann and David Ruelle. Ergodic theory of chaos and strange attractors. *Reviews of modern physics*, 57(July):617, 1985.
- [8] H. D. I. Abarbanel, R. Brown, and M. B. Kennel. Variation of lyapunov exponents on a strange attractor. *Journal of Nonlinear Science*, 1(2):175–199, 1991.
- [9] C. Nicolis, S. Vannitsem, and J.-F. Royer. Short-range predictability of the atmosphere: Mechanisms for superexponential error growth. *Quarterly Journal of the Royal Meteorological Society*, 121(523):705–722, 1995.
- [10] S. Vannitsem and C. Nicolis. Lyapunov vectors and error growth patterns in a t2113 quasigeostrophic model. *Journal of the Atmospheric Sciences*, 54(2):347 – 361, 1997.
- [11] L. De Cruz, S. Schubert, J. Demaeyer, V. Lucarini, and S. Vannitsem. Exploring the Lyapunov instability properties of high-dimensional atmospheric and climate models. *Nonlinear Processes in Geophysics*, 25(2):387–412, 2018.
- [12] Valerio Lucarini, Davide Faranda, Jorge Miguel Milhazes de Freitas, Mark Holland, Tobias Kuna, Matthew Nicol, Mike Todd, Sandro Vaienti, et al. *Extremes and recurrence in dynamical systems*. John Wiley & Sons, 2016.
- [13] Davide Faranda, Gabriele Messori, and Pascal Yiou. Dynamical proxies of north atlantic predictability and extremes. *Scientific reports*, 7(1):41278, 2017.

- [14] Assaf Hochman, Sebastian Scher, Julian Quinting, Joaquim G Pinto, and Gabriele Messori. Dynamics and predictability of cold spells over the eastern mediterranean. *Climate Dynamics*, 58(7):2047–2064, 2022.
- [15] Emma Holmberg, Gabriele Messori, Rodrigo Caballero, and Davide Faranda. The link between european warm-temperature extremes and atmospheric persistence. *Earth System Dynamics*, 14(4):737–765, 2023.
- [16] Gabriele Messori, Rodrigo Caballero, and Davide Faranda. A dynamical systems approach to studying midlatitude weather extremes. *Geophysical Research Letters*, 44(7):3346–3354, 2017.
- [17] Assaf Hochman, Gabriele Messori, Julian F Quinting, Joaquim G Pinto, and Christian M Grams. Do atlantic-european weather regimes physically exist? *Geophysical Research Letters*, 51(14), 2021.
- [18] Simon H Lee and Gabriele Messori. The dynamical footprint of year-round north american weather regimes. *Geophysical Research Letters*, 51(2):e2023GL107161, 2024.
- [19] Paul Platzer, Bertrand Chapron, and Pierre Tandeo. Dynamical properties of weather regime transitions. In *Stochastic Transport in Upper Ocean Dynamics Annual Workshop*, pages 223–236. Springer, 2021.
- [20] Guangpeng Liu, Fabrizio Falasca, and Annalisa Bracco. Dynamical characterization of the loop current attractor. *Geophysical Research Letters*, 48(24):e2021GL096731, 2021.
- [21] Adriano Gualandi, Luca Dal Zilio, Davide Faranda, and Gianmarco Mengaldo. Similarities and differences between natural and simulated slow earthquakes. *Geophysical Research Letters*, 48(20):e2021GL095574, 2024.
- [22] Davide Faranda, Gabriele Messori, Pascal Yiou, Soulihanh Thao, Flavio Pons, and Berengere Dubrulle. Dynamical footprints of hurricanes in the tropical dynamics. *Chaos: An Interdisciplinary Journal of Nonlinear Science*, 33(1), 2023.
- [23] Tommaso Alberti, Davide Faranda, Reik V Donner, Theophile Caby, Vincenzo Carbone, Giuseppe Consolini, Berengere Dubrulle, and Sandro Vaienti. Small-scale induced large-scale transitions in solar wind magnetic field. *The Astrophysical journal letters*, 914(1):L6, 2021.
- [24] Tommaso Alberti, Davide Faranda, Valerio Lucarini, Reik V Donner, Berengere Dubrulle, and François Davi-aud. Scale dependence of fractal dimension in deterministic and stochastic lorenz-63 systems. *Chaos: An Interdisciplinary Journal of Nonlinear Science*, 33(2), 2023.
- [25] Adriano Gualandi, J-P Avouac, Sylvain Michel, and Davide Faranda. The predictable chaos of slow earthquakes. *Science advances*, 6(27):eaaz5548, 2020.
- [26] V Slonosky and Pascal Yiou. Does the nao index represent zonal flow? the influence of the nao on north atlantic surface temperature. *Climate Dynamics*, 19(1):17–30, 2002.
- [27] Diego G Miralles, Adriaan J Teuling, Chiel C Van Heerwaarden, and Jordi Vilà-Guerau de Arellano. Mega-heatwave temperatures due to combined soil desiccation and atmospheric heat accumulation. *Nature geoscience*, 7(5):345–349, 2014.
- [28] Philipp Zschenderlein, Andreas H Fink, Stephan Pfahl, and Heini Wernli. Processes determining heat waves across different european climates. *Quarterly Journal of the Royal Meteorological Society*, 145(724):2973–2989, 2019.
- [29] Simone Russo, Jana Sillmann, and Erich M Fischer. Top ten european heatwaves since 1950 and their occurrence in the coming decades. *Environmental Research Letters*, 10(12):124003, 2015.
- [30] Marc Stefanon, Fabio D’ Andrea, and Philippe Drobinski. Heatwave classification over europe and the mediterranean region. *Environmental Research Letters*, 7(1):014023, 2012.
- [31] Assaf Hochman, Pinhas Alpert, Tzvi Harpaz, Hadas Saaroni, and Gabriele Messori. A new dynamical systems perspective on atmospheric predictability: Eastern mediterranean weather regimes as a case study. *Science advances*, 5(6):eaau0936, 2019.
- [32] Chenyu Dong, Davide Faranda, Adriano Gualandi, Valerio Lucarini, and Gianmarco Mengaldo. Revisiting the predictability of dynamical systems: a new local data-driven approach. *arXiv preprint arXiv:2409.14865*, 2024.
- [33] Davide Faranda, Gabriele Messori, Tommaso Alberti, Carmen Alvarez-Castro, Théophile Caby, Leone Cavicchia, Erika Coppola, Reik Donner, Berengere Dubrulle, Vera Melinda Galfi, et al. A statistical physics and dynamical systems perspective on geophysical extreme events. *arXiv preprint arXiv:2309.15393*, 2023.
- [34] George Datseris, Inga Kottlarz, Anton P Braun, and Ulrich Parlitz. Estimating fractal dimensions: A comparative review and open source implementations. *Chaos: An Interdisciplinary Journal of Nonlinear Science*, 33(10), 2023.
- [35] Keiron O’shea and Ryan Nash. An introduction to convolutional neural networks. *arXiv preprint arXiv:1511.08458*, 2015.



- [36] Yunjie Liu, Evan Racah, Joaquin Correa, Amir Khosrowshahi, David Lavers, Kenneth Kunkel, Michael Wehner, William Collins, et al. Application of deep convolutional neural networks for detecting extreme weather in climate datasets. *arXiv preprint arXiv:1605.01156*, 2016.
- [37] Jonathan A Weyn, Dale R Durran, and Rich Caruana. Improving data-driven global weather prediction using deep convolutional neural networks on a cubed sphere. *Journal of Advances in Modeling Earth Systems*, 12(9):e2020MS002109, 2020.
- [38] Ashesh Chattopadhyay, Ebrahim Nabizadeh, and Pedram Hassanzadeh. Analog forecasting of extreme-causing weather patterns using deep learning. *Journal of Advances in Modeling Earth Systems*, 12(2):e2019MS001958, 2020.
- [39] Ricardo García-Herrera, José Díaz, Ricardo M Trigo, Jürg Luterbacher, and Erich M Fischer. A review of the european summer heat wave of 2003. *Critical Reviews in Environmental Science and Technology*, 40(4):267–306, 2010.
- [40] Elisa Gallo, Marcos Quijal-Zamorano, Raúl Fernando Méndez Turrubiates, Cathryn Tonne, Xavier Basagaña, Hicham Achebak, and Joan Ballester. Heat-related mortality in europe during 2023 and the role of adaptation in protecting health. *Nature medicine*, pages 1–5, 2024.
- [41] Kristie L Ebi, Jennifer Vanos, Jane W Baldwin, Jesse E Bell, David M Hondula, Nicole A Errett, Katie Hayes, Colleen E Reid, Shubhayu Saha, June Spector, et al. Extreme weather and climate change: population health and health system implications. *Annual review of public health*, 42(1):293–315, 2021.
- [42] Daniela IV Domeisen, Elfatih AB Eltahir, Erich M Fischer, Reto Knutti, Sarah E Perkins-Kirkpatrick, Christoph Schär, Sonia I Seneviratne, Antje Weisheimer, and Heini Wernli. Prediction and projection of heatwaves. *Nature Reviews Earth & Environment*, 4(1):36–50, 2023.
- [43] S Pfahl and Heini Wernli. Quantifying the relevance of atmospheric blocking for co-located temperature extremes in the northern hemisphere on (sub-) daily time scales. *Geophysical Research Letters*, 39(12), 2012.
- [44] Christophe Cassou, Laurent Terray, and Adam S Phillips. Tropical atlantic influence on european heat waves. *Journal of climate*, 18(15):2805–2811, 2005.
- [45] B Legras and M Ghil. Persistent anomalies, blocking and variations in atmospheric predictability. *Journal of Atmospheric Sciences*, 42(5):433–471, 1985.
- [46] Davide Faranda, Giacomo Masato, Nicholas Moloney, Yuzuru Sato, Francois Daviaud, Bérengère Dubrulle, and Pascal Yiou. The switching between zonal and blocked mid-latitude atmospheric circulation: a dynamical system perspective. *Climate Dynamics*, 47:1587–1599, 2016.
- [47] Valerio Lucarini and Andrey Gritsun. A new mathematical framework for atmospheric blocking events. *Climate Dynamics*, 54(1):575–598, 2020.
- [48] Sebastian Schubert and Valerio Lucarini. Dynamical analysis of blocking events: spatial and temporal fluctuations of covariant lyapunov vectors. *Quarterly Journal of the Royal Meteorological Society*, 142(698):2143–2158, 2016.
- [49] Hans Hersbach, Bill Bell, Paul Berrisford, Shoji Hirahara, András Horányi, Joaquín Muñoz-Sabater, Julien Nicolas, Carole Peubey, Raluca Radu, Dinand Schepers, et al. The era5 global reanalysis. *Quarterly Journal of the Royal Meteorological Society*, 146(730):1999–2049, 2020.
- [50] Aglaé Jézéquel, Pascal Yiou, and Sabine Radanovics. Role of circulation in european heatwaves using flow analogues. *Climate dynamics*, 50(3):1145–1159, 2018.
- [51] Christophe Cassou and Julien Cattiaux. Disruption of the european climate seasonal clock in a warming world. *Nature Climate Change*, 6(6):589–594, 2016.
- [52] Daniel S Wilks. “the stippling shows statistically significant grid points”: How research results are routinely overstated and overinterpreted, and what to do about it. *Bulletin of the American Meteorological Society*, 97(12):2263–2273, 2016.
- [53] Zsuzsanna RÁCZ and Roger K Smith. The dynamics of heat lows. *Quarterly Journal of the Royal Meteorological Society*, 125(553):225–252, 1999.
- [54] Tim Woollings, David Barriopedro, John Methven, Seok-Woo Son, Olivia Martius, Ben Harvey, Jana Sillmann, Anthony R Lupo, and Sonia Seneviratne. Blocking and its response to climate change. *Current climate change reports*, 4:287–300, 2018.
- [55] Lisa-Ann Kautz, Olivia Martius, Stephan Pfahl, Joaquim G Pinto, Alexandre M Ramos, Pedro M Sousa, and Tim Woollings. Atmospheric blocking and weather extremes over the euro-atlantic sector—a review. *Weather and Climate Dynamics Discussions*, 2021:1–43, 2021.

- [56] Lukas Brunner, Nathalie Schaller, James Anstey, Jana Sillmann, and Andrea K Steiner. Dependence of present and future european temperature extremes on the location of atmospheric blocking. *Geophysical research letters*, 45(12):6311–6320, 2018.
- [57] Vera Melinda Galfi and Valerio Lucarini. Fingerprinting Heatwaves and Cold Spells and Assessing Their Response to Climate Change Using Large Deviation Theory. *Phys. Rev. Lett.*, 127:058701, Jul 2021.
- [58] Valerio Lucarini, Vera Melinda Galfi, Jacopo Riboldi, and Gabriele Messori. Typicality of the 2021 Western North America summer heatwave. *Environmental Research Letters*, 18(1):015004, jan 2023.
- [59] E. M. Fischer, U. Beyerle, L. Bloin-Wibe, C. Gessner, V. Humphrey, F. Lehner, A. G. Pendergrass, S. Sippel, J. Zeder, and R. Knutti. Storylines for unprecedented heatwaves based on ensemble boosting. *Nature Communications*, 14(1):4643, 2023.
- [60] Vera Melinda Gálfi, Valerio Lucarini, Francesco Ragone, and Jeroen Wouters. Applications of large deviation theory in geophysical fluid dynamics and climate science. *La Rivista del Nuovo Cimento*, 44(6):291–363, 2021.
- [61] Giovanni Dematteis, Tobias Grafke, and Eric Vanden-Eijnden. Rogue waves and large deviations in deep sea. *Proceedings of the National Academy of Sciences*, 115(5):855–860, 2018.
- [62] Laura Ferranti, Susanna Corti, and Martin Janousek. Flow-dependent verification of the ecmwf ensemble over the euro-atlantic sector. *Quarterly Journal of the Royal Meteorological Society*, 141(688):916–924, 2015.
- [63] Athony Leonard. Energy cascade in large-eddy simulations of turbulent fluid flows. In *Advances in geophysics*, volume 18, pages 237–248. Elsevier, 1975.
- [64] Christophe Cassou. Intraseasonal interaction between the madden–julian oscillation and the north atlantic oscillation. *Nature*, 455(7212):523–527, 2008.

## Supplementary Information

### Text S1. Dynamical Indices

In this section of the supplementary text, we expand on the definition of instantaneous dimension ( $d$ ) and inverse persistence ( $\theta$ ) used in the main text. As introduced in the main text, these two dynamical indices grounded at the intersection of dynamical systems theory and extreme value theory, and were developed by [12] and [13] to characterize local dynamical properties of complex systems. For one given state of interest  $\zeta$  in the phase space, this methodology uses its neighboring states, also known as *recurrences*, to derive its state-dependent dynamical properties. Specifically, for the considered state  $\zeta$ , we first calculate its negative logarithmic distances to other states:

$$g(\zeta, \mathbf{x}(t)) = -\log [\text{dist}(\mathbf{x}(t), \zeta)], \quad (1)$$

where  $\mathbf{x}(t)$  is the trajectory of the studied system and the *dist* function can be any distance metric. Requiring a trajectory falls within a neighborhood of  $\zeta$  (a hypersphere in the phase space) is a synonym of having the time series  $g[\zeta, \mathbf{x}(t)]$  above one threshold  $s(q, \zeta)$ , where  $s(q, \zeta)$  is a high threshold associated with a quantile  $q$  of the series  $\mathbf{X} \equiv g(\zeta, \mathbf{x}(t))$  ( $q$  is chosen as a high value to identify neighboring states). Then, we define a quantity called *exceedance* for the neighboring states (i.e., recurrences) of  $\zeta$  as follows:

$$\mathbf{u}(\zeta) = g(\zeta, \mathbf{x}(t)) - s(q, \zeta), \quad \forall g(\zeta, \mathbf{x}(t)) > s(q, \zeta) \quad (2)$$

According to extreme value theory, under the assumption of independent exceedances, the cumulative probability distribution  $F(\mathbf{u}, \zeta)$  follows the exponential form of the generalized Pareto distribution (GPD), expressed as:

$$F(\mathbf{u}, \zeta) \sim \exp \left[ -\frac{\mathbf{u}(\zeta)}{\sigma(\zeta)} \right]. \quad (3)$$

The scale parameter  $\sigma(\zeta)$  of the distribution depends on the state  $\zeta$  and can be utilized to compute the local dimension as  $d(\zeta) = 1/\sigma(\zeta)$ , in accordance to its definition. The local dimension  $d$  serves as an indicator of the number of active degrees of freedom in the system in the vicinity of  $\zeta$ . Consequently, it captures the complexity of the dynamics near the state  $\zeta$ : a system with a greater number of active degrees of freedom exhibits higher complexity.

For the other local index, inverse persistence  $\theta$ , its definition is adopted from the extremal index in extreme value theory. This dimensionless parameter quantifies the inverse of the clustering duration of extremes. In this context, extremes are defined as recurrences within the neighborhood of the reference state  $\zeta$ . Consequently, persistence ( $\theta^{-1}$ ) represents the average number of consecutive recurrences, thereby providing insight into the system's instantaneous persistence. Unlike the local dimension ( $d$ ), which requires *exceedances* for its estimation, the inverse persistence ( $\theta$ ) is derived solely from the chronological order of *recurrences* of the reference state  $\zeta$ . The full mathematical derivation of these two indices can be found in [33].

### Text S2. Definition of European Regional Heatwaves

We define regional warm-temperature extremes over the British Isles, Scandinavia, central Europe (Germany), Iberia, and the central Mediterranean for extended summer season (JJAS), following the bounding boxes used in [28].

To this end, we first define two criteria for each individual grid point using ERA5 daily maximum 2-meter temperature data from 1979 to 2022, following [29]. The first criterion requires the daily maximum temperature to exceed a threshold, defined as the 90th percentile of the daily maximum temperature for that calendar day, calculated using a centered 15-day window. The second criterion requires  $M_d > 0$ , where  $M_d$  is a daily heatwave magnitude index defined as:

$$M_d = \begin{cases} \frac{T_d - T_{30y,25p}}{T_{30y,75p} - T_{30y,25p}}, & \text{if } T_d > T_{30y,25p}, \\ 0, & \text{if } T_d \leq T_{30y,25p}. \end{cases} \quad (4)$$

with  $T_d$  being the daily maximum 2-meter temperature data and  $T_{30y,75p}$  ( $T_{30y,25p}$ ) denotes the 75th (25th) percentile of annual maximum temperatures within a 30-years sliding window. Subsequently, we aim to exclude events that are either very localized or short-lived. Accordingly, we define heatwave events as those in which at least 5% of the predefined region (see solid boxes in Figure 2) simultaneously meet the two criteria outlined above and persist for a minimum of three consecutive days. Heatwave onset days used in this study are then identified as the first days of these events.

### Text S3. Definition of Atmospheric Blocking events

In this study, we primarily focus on the dynamical properties of atmospheric circulation patterns associated with European summertime heatwaves from a dynamical systems theory perspective. However, we note that another discrepancy in existing studies lies in the characterization of atmospheric blocking. While the traditional meteorological perspective considers it a highly persistent and stable configuration [45], conclusions derived from dynamical systems theory suggest otherwise [13].

We aim to address this discrepancy using analysis based on our novel framework. Nonetheless, acknowledging that heatwaves are not systematically associated with blocking events [55], such a conclusion cannot be drawn from the results presented in the main text. Therefore, we employ a blocking detection algorithm to rigorously define these events and, based on this, attempt to reconcile the aforementioned discrepancy.

We applied a standard blocking detection algorithm based on the reversal of 500-hPa geopotential height gradients, as described by [56] and references therein. For each grid point, we first compute its geopotential height gradients to the north ( $\Delta Z_N$ ) and to the south ( $\Delta Z_S$ ):

$$\begin{aligned} \Delta Z_N &= \frac{Z(\lambda, \phi + \Delta\phi) - Z(\lambda, \phi)}{\Delta\phi} \\ \Delta Z_S &= \frac{Z(\lambda, \phi) - Z(\lambda, \phi - \Delta\phi)}{\Delta\phi} \end{aligned} \quad (5)$$

where  $Z$  represents geopotential height at 500-hPa,  $\Delta\phi = 15^\circ$ , and  $\phi$  ranges from  $50^\circ N$  to  $75^\circ N$ . Instantaneous blocking (IB) is defined at a specific grid point if the gradients simultaneously satisfy the following conditions:

$$\Delta Z_N < -10m/(\text{°lat}); \Delta Z_S > 0m/(\text{°lat}) \quad (6)$$

Next, we apply spatiotemporal filtering to the IB field to extract large-scale and slow-moving events. The maximum IB index within  $\pm 4^\circ$  latitude is taken to account for meridional movement. Extended IB cases are then selected if they span at least  $15^\circ$  longitude, filtering out systems that are too small. Finally, blocking is defined as an extended IB persisting within  $\pm 10^\circ$  longitude for at least five consecutive days, ensuring the detection of only persistent and slow-moving systems.

Blocked days are further determined for three  $30^\circ$  longitude regions, namely Greenland ( $60^\circ W$  to  $30^\circ W$ ), North Atlantic ( $30^\circ W$  to  $0^\circ$ ), and Scandinavian ( $0^\circ$  to  $30^\circ E$ ). A day is considered blocked in a given region if a block spans more than half of the region (i.e., exceeds  $15^\circ$  of longitude within the region). Based on this, we can plot the composite anomalies of the standardized anomalies for blocked days within the three regions, as shown in Fig. 10.

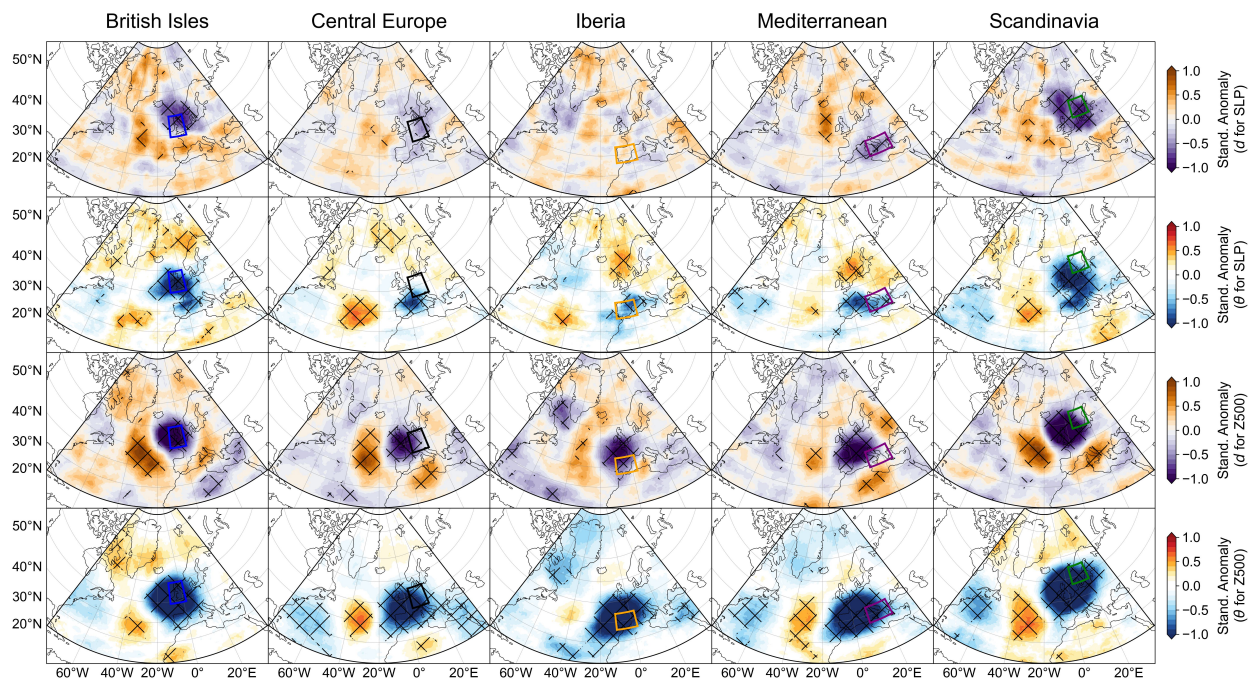


Figure 5: Composite of standardized anomalies of dynamical indices for the onset days of European summertime heatwaves. As in Fig. 2, but for dynamical indices based on smaller window size (20° longitude by 10° latitude).

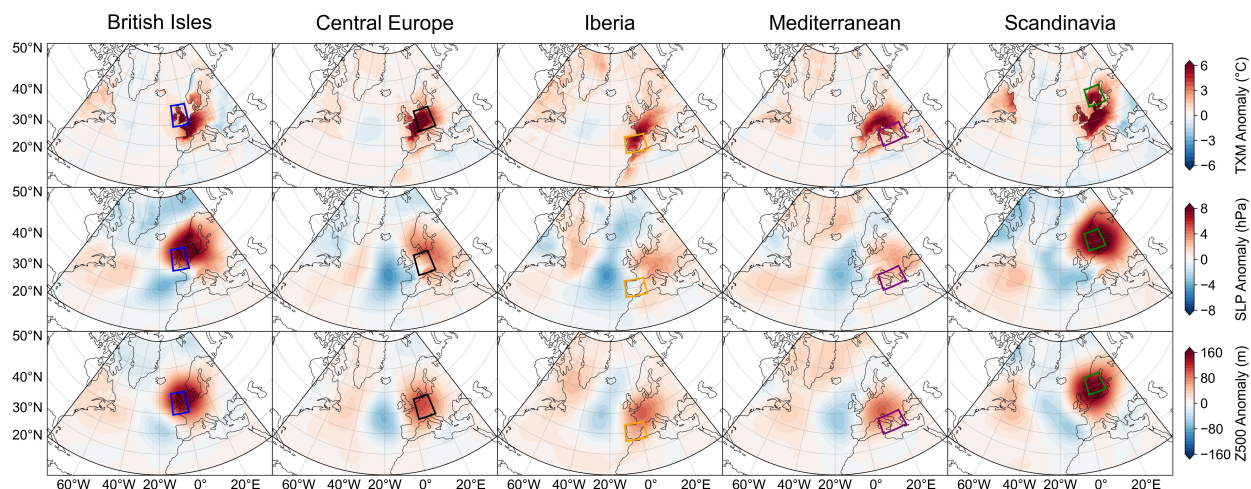


Figure 6: Onset patterns of European summertime heatwaves. Composite anomalies for the onset days of summertime heatwaves across Europe: daily maximum 2-meter temperature (row 1), sea level pressure (row 2), and 500 hPa geopotential height (row 3).



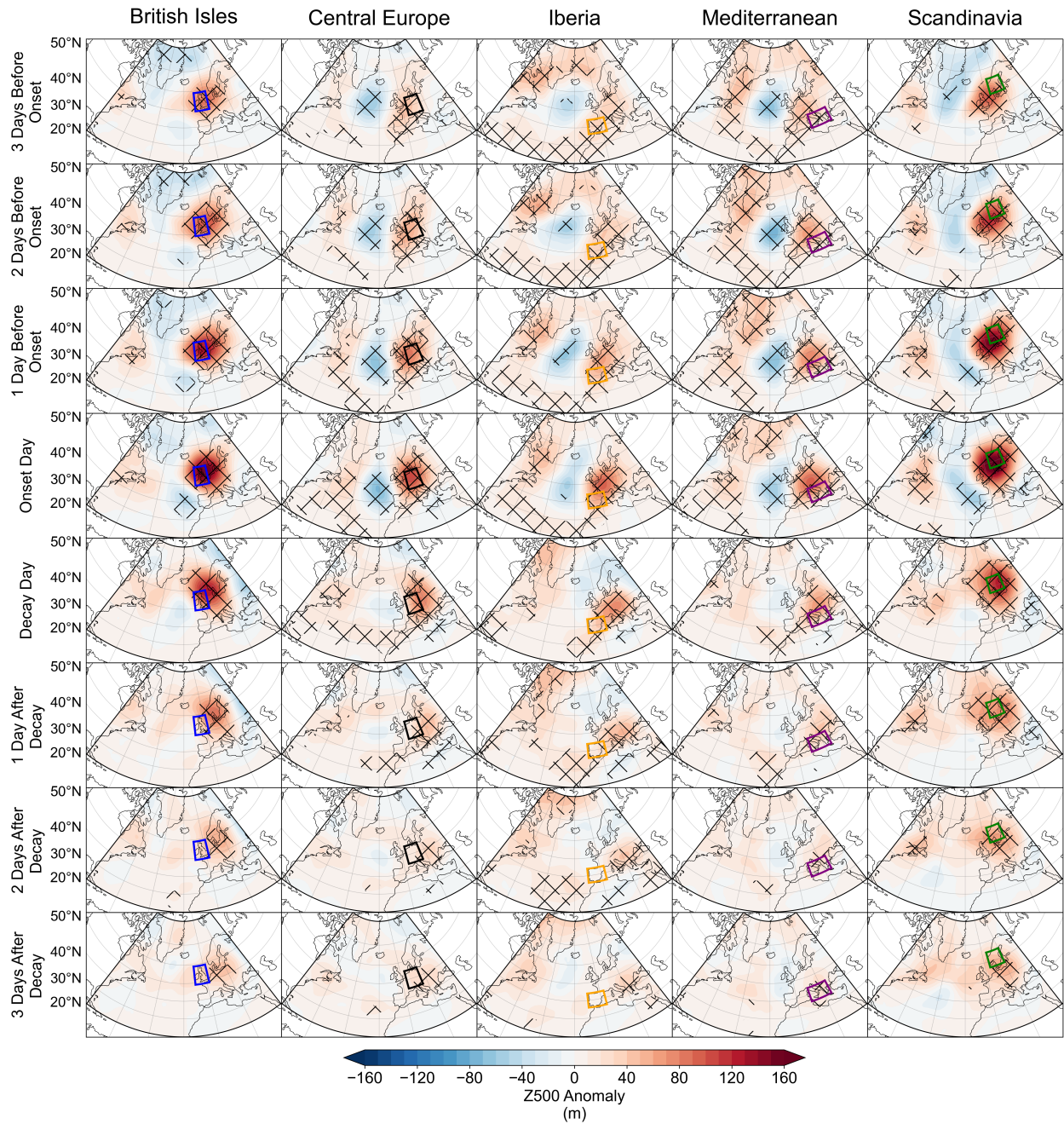


Figure 7: **Temporal evolution of the composite anomaly of Z500 before the onset and after the decay of European summertime heatwaves.** Composite anomaly of Z500 from three days before the onset to the onset day, and from the last day to three days after, of summertime heatwaves across Europe.

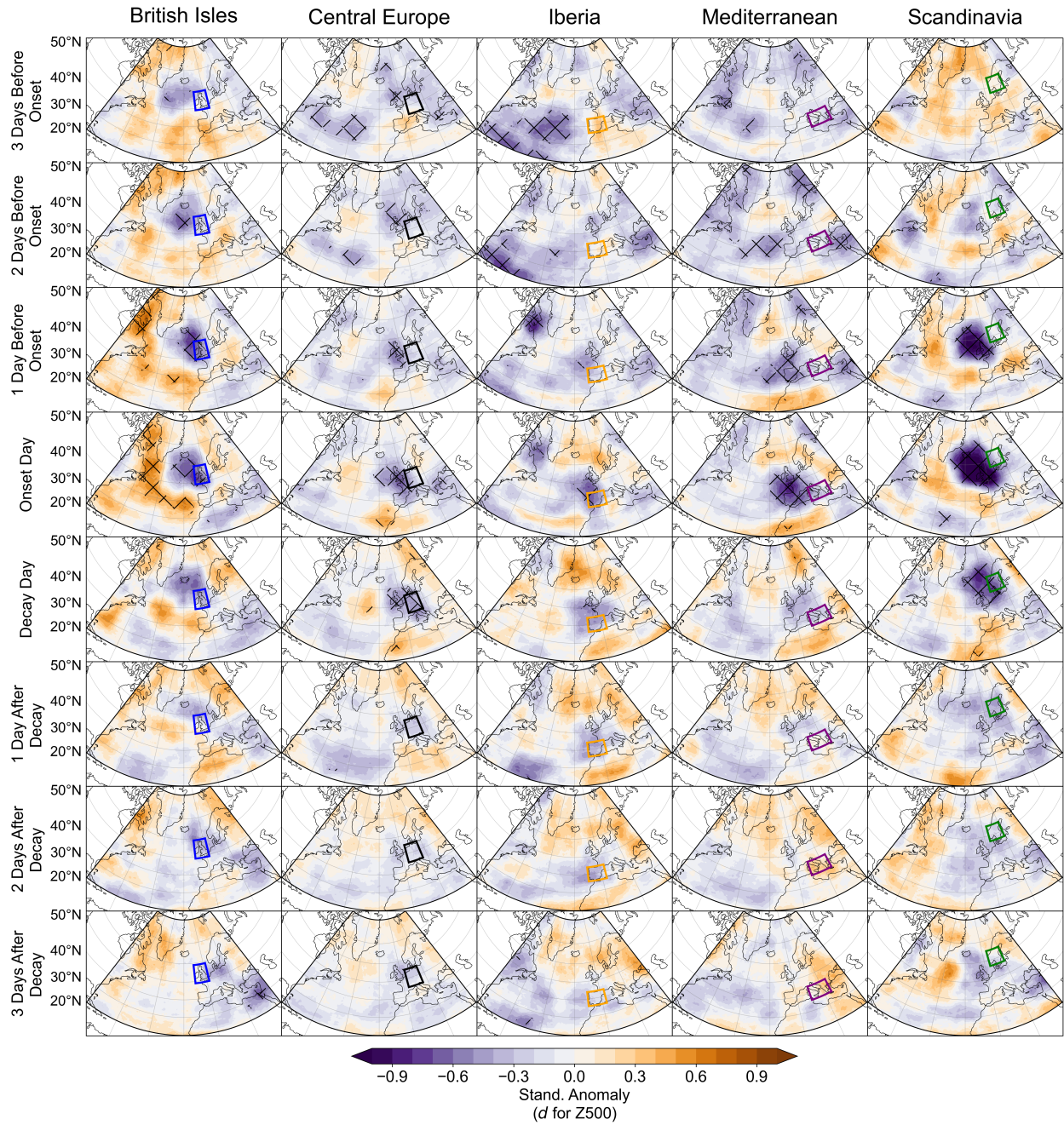


Figure 8: **Temporal evolution of the composite anomaly of Z500-based local dimension ( $d$ ) before the onset and after the decay of European summertime heatwaves.** As in Fig. S3, but for Z500-based local dimension.



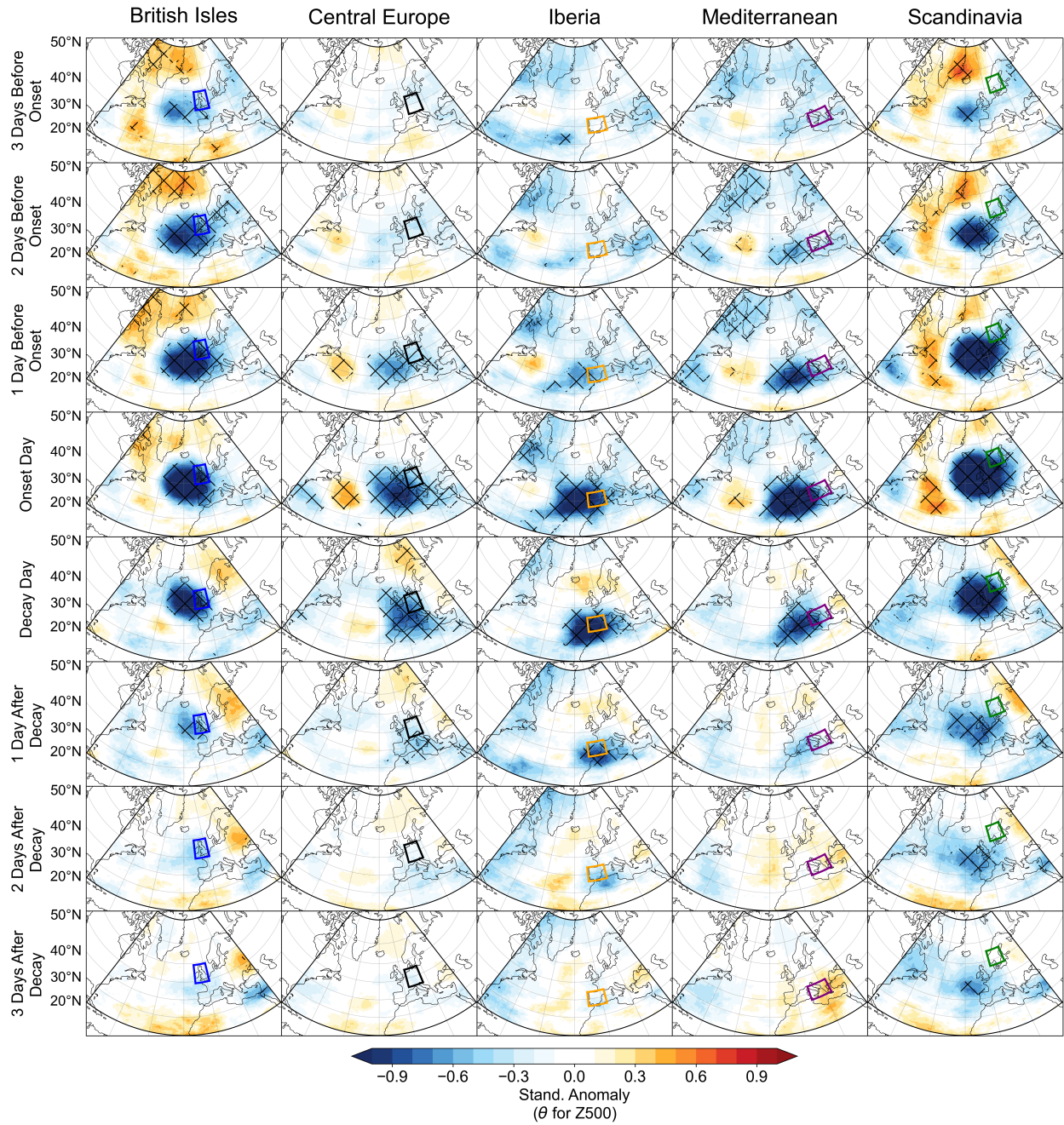


Figure 9: Temporal evolution of the composite anomaly of Z500-based inverse persistence ( $\theta$ ) before the onset and after the decay of European summertime heatwaves. As in Fig. S3, but for Z500-based inverse persistence.



### Composite Anomalies for Summertime Blocking

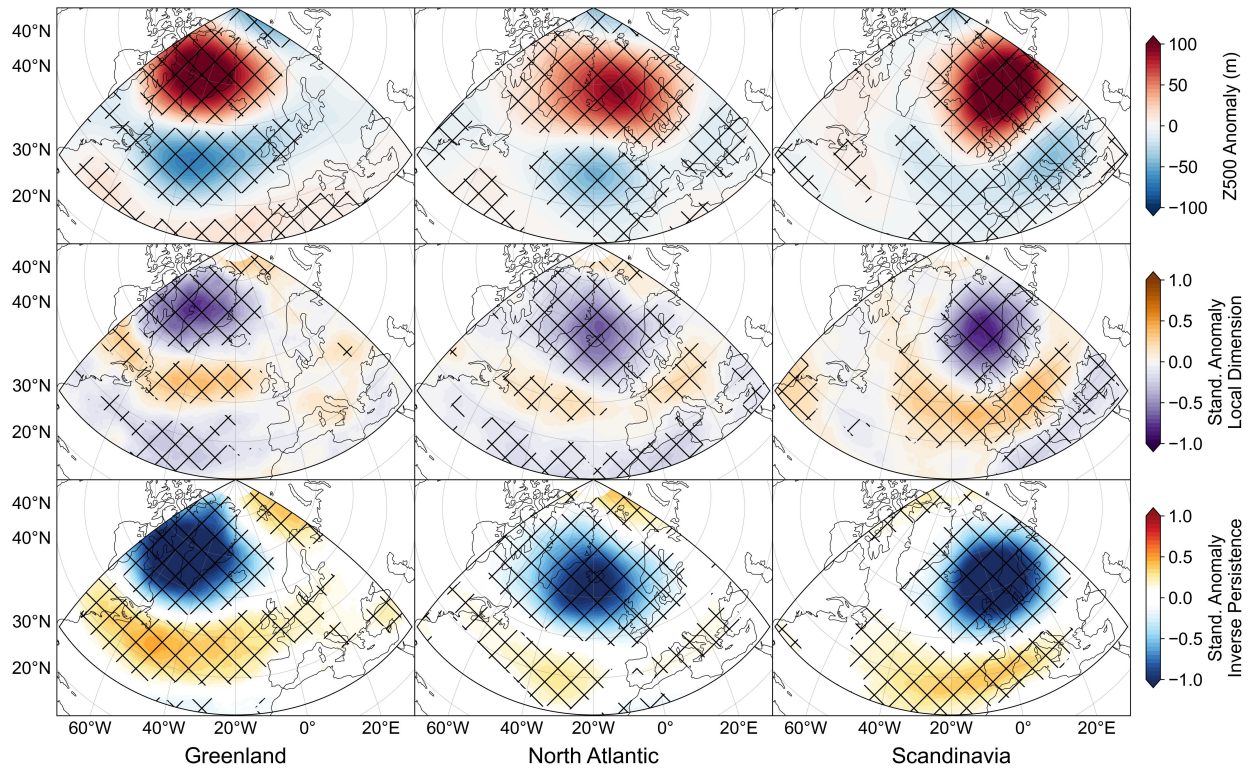


Figure 10: **Composite anomalies for atmospheric blocking events.** Composite anomaly of the 500 hPa geopotential height for atmospheric blocking at different locations in the Euro-Atlantic sector (row 1). Composite of standardized anomalies for the local dimension  $d$  (row 2) and the inverse persistence  $\theta$  (row 3) that were computed using 500 hPa geopotential height.